Accurate Estimation of Passive Component Defect and Degradation in DC-DC Power Converters from Transient Terminal Responses

T. J. Rosenthal, J. L. Rio, O. O. Olagbemi, P. Gómez

***Abstract*—DC-DC power converters are experiencing an exponential increase in their utilization with the grid interconnection of distributed energy resources, electric vehicles, and energy storage units. Thus, their appropriate operation under different conditions is crucial. This depends largely on the use of reliable inductors and capacitors to maintain output quality and power efficiency. However, deterioration or damage of these components over time is inevitable. In this paper, we propose the use of transient terminal measurements of voltage and current to estimate deterioration or formation of defects in inductive and capacitive components of buck and boost power converters. Our method involves the application of the numerical Laplace transform to define an algebraic system of equations. An approximate solution for the converter's two-port model is then related to the specific inductive and capacitive parameters of the reconstructed model. Variations in these parameters due to deterioration/damage conditions are simulated using finite element analysis and analytical approximations. The results for the test cases presented demonstrate the effectiveness of the proposed method to accurately estimate converter parameter variation under different conditions.**

***Keywords*: DC-DC power converter, parameter estimation, parametric fault detection, transient measurements.**

I. Introduction

POWER converters are the gateways for the interconnection of generation systems, microgrids, electric vehicles, battery storage units, and other distributed energy resources (DERs) to the power grid, as well as for HVDC systems, transportation electrification, industrial-grade motor drives, among many other AC/DC systems at high-, medium- and low-voltage levels [1], [2].

Estimating the reliability and life expectancy of power converters is paramount for decision-making and planning in modern power-electronic based systems [1]. Power converters are considered a weak link that can have a substantial impact on the overall system reliability [3]. For instance, it is estimated that power converters are responsible for 13% of failures and 18% of downtime in wind farms, and 37% of unscheduled maintenance in utility scale photovoltaic systems [3].

Inductor, capacitor and semiconductive component damages are listed among the main contributors to faults in power-electronic conversion systems [4]. From these elements, capacitors are considered the most critical components to converters' reliability given their high degradation failure rate. Approximately 30% of converter failures are associated with capacitor degradation [5].

Faults in power-electronic converters can be classified into hard faults and soft faults. Hard faults occur when an event, such as a short circuit or an open circuit, produces complete damage of a component. Soft faults happen when partial damage, deterioration or aging results in a parametric variation of main components, such as a decrease in the value(s) of the converter's inductor(s), capacitor(s), or the modification of the operational characteristics of a semiconductive switch (e.g., input impedance or on-state conduction losses) [6]. Over time, soft faults can evolve into hard faults, so their timely detection is very important to ensure the reliable operation of power converters.

Fault detection methods for DC-DC converters are classified into model-based methods, signal-based methods, knowledge-based methods (a.k.a. data-driven methods) and hybrid methods [6]-[8]. Model-based methods, such as the ones proposed in [6], [9], [10] require the availability of a mathematical model of the system from physical principles or system identification, which can be a complicated task depending on the converter's topology [7]. Signal-based methods (e.g., [11], [12]) use measured signals that can be directly related to specific faulty conditions. These signals can be in time domain, frequency domain, or both. However, these methods may struggle to differentiate signals from healthy and faulty conditions depending on the type and number of signals recorded [7]. In contrast to the two previous methods, knowledge-based methods (see for instance [13]-[15]) do not require a previously known model or signal pattern of the system under study. Instead, a large volume of historic data is obtained, and AI techniques are then applied to these data to systematically extract the implicit fault characteristics of the system. A main limitation of this method is the need to record large amounts of data and utilize computationally expensive techniques for the training process [8]. Finally, hybrid methods combine two or more fault detection methods [8].

This work was supported by the Research Experiences for Undergraduates (REU) Program and the Engineering Research Initiation (ERI) Program, both of the National Science Foundation (NSF), under grants #2244390 and #2138408, respectively.

T. J. Rosenthal is with Valparaiso University, Valparaiso, IN 46383 USA (e-mail: trent.rosenthal@valpo.edu).

J. L. Rio is with City Colleges of Chicago, Chicago, IL 60634 USA (e-mail: rio5@illinois.edu).

O. O. Olagbemi and P. Gómez are with Western Michigan University, Kalamazoo, MI 49008 USA (e-mail: pablo.gomez@wmich.edu).

Paper submitted to the International Conference on Power Systems Transients (IPST2025) in Guadalajara, Mexico, June 8-12, 2025.

In this paper, we aim to contribute to the current state of the art on power converter soft fault detection by proposing and evaluating a novel hybrid (model-based and signal-based) frequency-domain approach to estimate parameter variation due to soft faults on passive components of DC-DC buck and boost converters. Building upon our previous work [16], our proposed method utilizes transient terminal measurements of voltage and current to estimate deterioration or formation of defects in inductive and capacitive components. This involves the application of the numerical Laplace transform [17] to define an algebraic system of equations and approximate its solution for the converter's two-port model, which is then related to the specific inductive and capacitive parameters of the reconstructed model by comparing it with an approximate mathematical model of the converter.

Considering existing methods and approaches, the following salient features of our proposed method include:

1. Very low computational burden compared with existing data-driven methods, given that it requires only four sets of transient response measurements. It also avoids the need for computationally intensive and time-consuming data training.
2. Very straightforward algebraic model definition and solution due to the use of a Laplace-domain two-port representation.

The remainder of our paper is structured as follows: Section II describes the general methodology proposed. Section III details the approach followed to simulate passive component defect and degradation. Section IV illustrates the generation of transient measurements with varying L-C values. Section V shows the application of the proposed method for several test cases and discusses the results obtained. Finally, the conclusions of this paper are included in Section VI.

II. General Methodology

Our proposal involves the following main components:

1. Approximating inductive and capacitive parameter variation due to deterioration or defect.
2. Utilizing a switching model of the converter under study to simulate a series of transient responses as a function of inductive and/or capacitive variation.
3. Transforming the transient responses obtained above to the Laplace domain in order to define an algebraic system of equations solved for the two-port model of the converter.
4. Relating the two-port model obtained to the inductive and capacitive values for the converter under study.

The block diagram in Fig. 1 illustrates the process followed. These steps are explained in detail in the next sections of the paper. The light blue rectangles correspond to stages that are only necessary in this work to emulate the terminal measurements of converters. In a practical application, these steps would be replaced by the use of real (measured) converter responses to estimate the level of component defect or degradation, as shown in the last stage of the diagram (in light green).

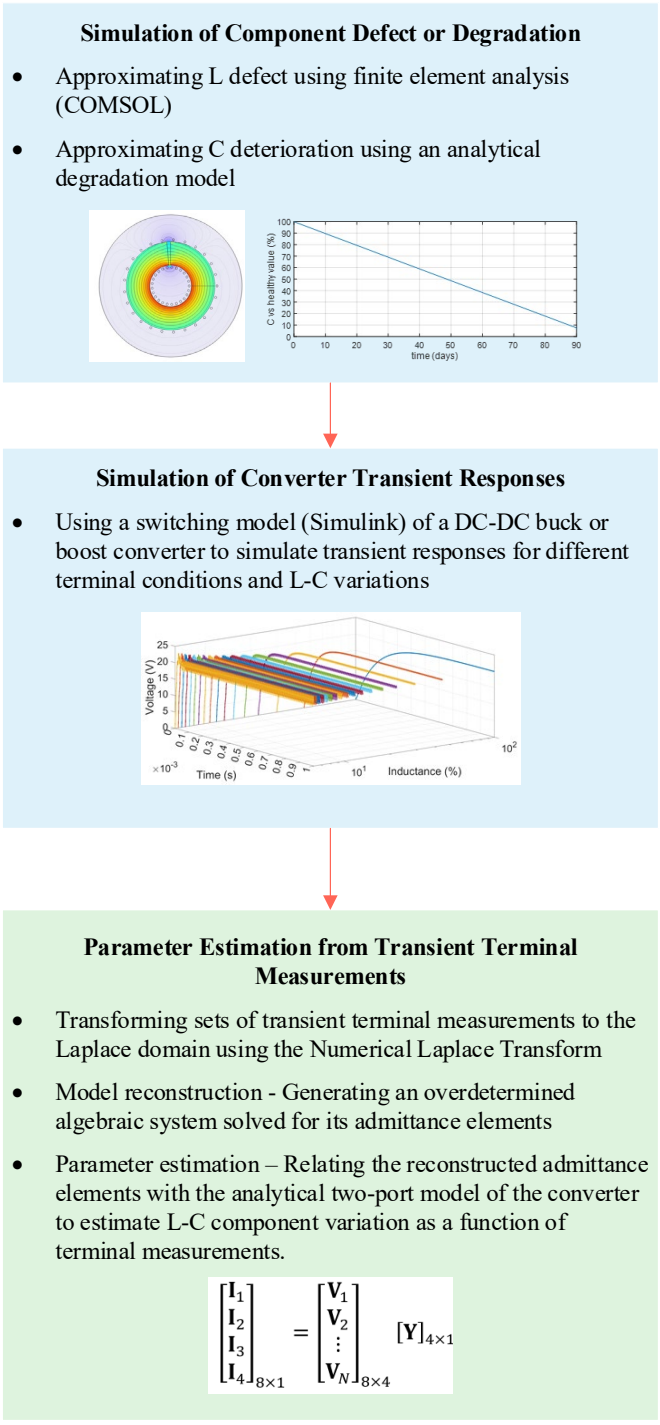

Fig. 1. Block diagram illustrating the general methodology.

III. Simulation of Component Defect or Degradation

This is performed using finite element analysis in the case of inductors, and an analytical approximation in the case of capacitors.

A. Inductor defect analysis

This work assumes the use of a toroidal geometry for the converter's inductive component. However, other inductor topologies can be considered following a similar approach.

Before introducing a defect, healthy inductance values are

calculated based on well-known design formulas for buck and boost converters [18], [19] and the sample parameters listed in Table I, which are selected only for demonstration purposes.

For the buck converter, this calculation results in an approximate inductance of 3 mH, while a value of 1 mH is obtained for the boost converter. Practical toroidal core topologies to achieve these values are found from manufacturer datasheets [20], [21], resulting in the materials and dimensions listed in Tables II and III.

TABLE I
DC-DC BUCK AND BOOST CONVERTER PARAMETERS

Nominal Parameters	Buck	Boost
Input voltage, V_{in}	220 V	200 V
Output voltage, V_{out}	55 V	333.33 V
Duty cycle, D_c	0.25	0.4
Switch frequency, f_s	100 kHz	100 kHz
Nominal load, R_L	10 Ω	10 Ω
Max. permissible steady-state current ripple	5%	5%
Max. permissible steady-state voltage ripple	5%	5%

TABLE II
DC-DC CONVERTER INDUCTOR MODEL DIMENSIONS

Dimension	Buck	Boost
	value [mm]	
Outer core radius	12.1319	24.8
Inner core radius	6.7528	11.624
Coil wire radius	0.4572	0.6
Core depth	18.796	22
Surrounding space (for simulation)	15	40
No. turns	30 turns	25 turns

TABLE III
DC-DC CONVERTER INDUCTOR MATERIALS

		Buck	Boost
Region	Material	Relative permeability	
Surrounding space / fracture	Air	1	
Core	Alloy	1513.47	480
Coil	Copper	1	

Two types of inductor core defects are considered: widening fracture and deepening fracture. Given the typical materials used in toroidal inductors for high frequency applications (e.g., ferrite, powdered iron, amorphous alloy, nanocrystalline), these defects can happen over time due to weather variations, vibration, transport, or other circumstances.

A widening fracture is a complete fracture across the radial length of the core. This was simulated using COMSOL Multiphysics [22] and its "parametric sweep" capabilities, with a varying size defined by an angle with respect to a vertical starting line of the fracture, defining the relative permeability of the fractured segment as 1, in contrast to the high relative permeability of the core (1513.47 for the buck converter's inductor and 480 for the boost converter's inductor, as listed in Table III). A sample COMSOL simulation for this case is shown in Fig. 2(a). Fig. 3(a) shows the effect of the gap size for the two inductors considered. The inductance behavior is exponentially decreasing in both cases. With a gap of only 1°, the inductor value decreases to 20.78% of its original value for the buck converter and 44.84% for the boost converter.

The second defect evaluated is a deepening fracture. This is a partial fracture where a fixed gap angle is assumed as shown in Fig. 2(b). Using parametric sweep, the depth of the fracture is modified to evaluate the effect of the size of the partial defect. Fig. 3(b) shows the effect of varying the partial gap size for the two inductors under evaluation. In this case the behavior of the inductance value is logarithmically decreasing in both cases, since the flow of magnetic field in the core material is only partially disrupted.

It is important to note that, in practice, core defects are much more complex in nature than our simulations. However, our simulations still allow us to consider, in a simplified manner, the inductance decrease for different types of defects and levels of severity, which is then used in the proposed parameter estimation approach. More realistic defect simulation is out of the scope of the present study and can be a matter of future research.

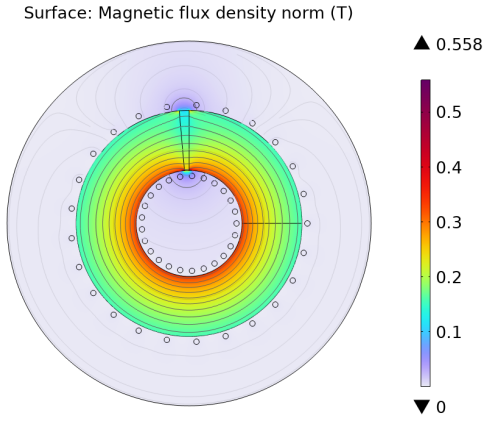

(a)

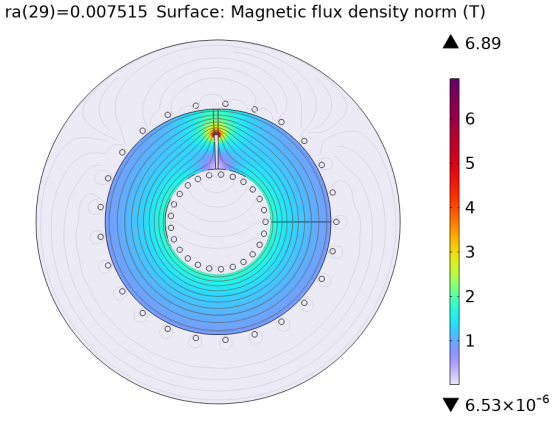

(b)

Fig. 2. 2D finite element model of toroidal inductor for two types of core defects: (a) complete fracture, (b) partial fracture.

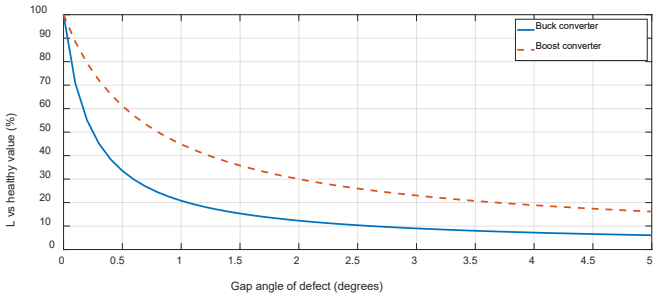

(a)

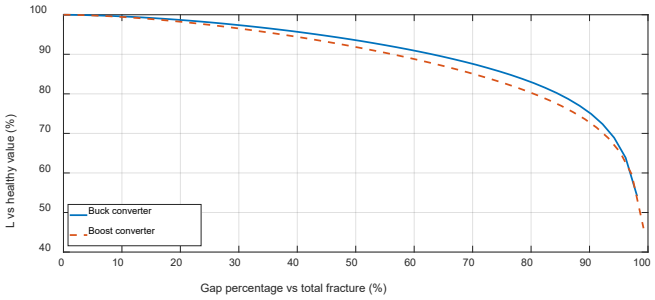

(b)

Fig. 3. Decrease of inductance as defect increases: (a) complete fracture, (b) partial fracture.

B. Capacitor degradation analysis

We assume the use of an electrolytic capacitor for both converters under study. Other types of capacitors and degradation models can be considered following a similar approach [23].

First, initial (healthy) capacitive values were calculated based on well-known design formulas for buck and boost converters [18], [19] and the sample parameters listed in Table I. This resulted in values of 1.5 µF for the buck converter and 40 µF for the boost converter.

The capacitor degradation model applied here is based on the following expressions [24]:

$$C(t) = C_0(1 + A\,t), \tag{1}$$

$$A = A_0 e^{\frac{-E_{a1}}{\kappa T}}, \tag{2}$$

where C_0 is the initial (healthy) capacitance value, t is the time in seconds, A_0 is the base degradation rate, E_{a1} is the activation energy, κ is the Boltzmann constant, and T is the temperature in Kelvin. Based on [24], some considerations were made for these values to simulate a defective electrolytic capacitor whose value would decrease to 7.5% of its healthy value after only 90 days of continuous operation: temperature of 293 K (19.85 °C), base degradation rate of -3.5×10^6 and activation energy of 0.783 eV. This resulted in the linear decrease shown in Fig. 4.

The parameters of the electrolytic capacitor degradation model defined in (1) and (2) are typically determined experimentally, applying a fitting method (such as the least squares method) to fit the experimental data at various temperatures. More details of experimental data analysis, test procedures, and fitting analysis are provided in [25].

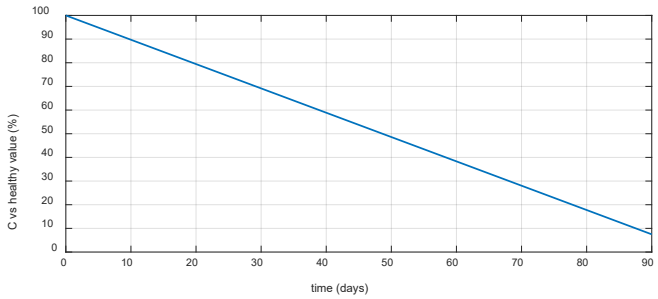

Fig. 4. Decrease of capacitance with time for defective component

IV. Simulation of Converter Transient Responses under Varying Terminal Conditions and L-C Values

Synchronous DC-DC converter models were implemented in Simulink [26] (one for buck converter and another for boost converter) with varying terminal (source-load) conditions, thus producing different transient voltage and current responses. For *N* different terminal conditions, *N* distinct sets of emulated terminal voltage and current measurements are generated. These measurement sets are the basis of the parameter estimation method, as explained in Section VI of this paper.

The basic DC-DC converter model in Simulink corresponds to a synchronous switching model with two semiconductive switches operating alternatively, an inductor and a capacitor. Buck and boost converter topologies include the same switching elements but in different positions. The model is terminated in a DC voltage source and a resistive load.

Four distinct responses (measurement sets) are generated per inductance value, considering variation of DC voltage source magnitude and resistive load as follows: 160 V – 1 Ω, 220 V – 12 Ω, 120 V – 5 Ω, and 80 V – 20 Ω, as proposed in [16]. Depending on the specific converter under study, these tests will change to reflect diverse source and load conditions within the operational range of the device.

Initial inductive and capacitive values correspond to healthy components, which are then varied to simulate the effect of component defect or degradation. As an example, Fig. 5 shows the effect of inductance decrease due to a widening defect on the output voltage and inductor current responses of the buck converter. Both responses show an evident increase in ripple content and transient overshoot, as well as faster response time, with the decrease of inductance as the widening defect becomes more evident. This example corresponds to the measurement set with input voltage magnitude of 80 V and output resistance of 20 Ω, but a similar change in behavior with inductance value is present for all four measurement sets considered. Notice that the axis corresponding to inductance percentage has a logarithmic scale given the type of inductance decrease present in this case.

A second example shows the effect of capacitor deterioration on the output voltage of the buck converter, combined with a partial inductor core fracture. For this example, the capacitor degradation model parameters are set up to consider a defective electrolytic capacitor that would decrease its value to approximately 7.5% of its original

(healthy) value after only 90 days of continuous operation, as explained in Section III.B. In addition, the inductance is fixed at 1/3 of its healthy value to consider a partially fractured component. The plot in Fig. 6 shows the output voltage of the buck converter for different capacitor values starting with its healthy value of 1.5 μF. An increase in ripple content with capacitor deterioration level is observed. This example also corresponds to the 80 V – 20 Ω measurement set.

V. Parameter Estimation from Transient Terminal Responses

The use of transient terminal responses of voltage and current for parameter defect estimation is the central part of the present proposal. The main idea is the generation of an algebraic system that uses N distinct sets of (input/output) terminal voltage and current responses of the DC-DC converter to estimate the L-C parameters of the converter generating such responses. Furthermore, estimation of such parameters serves as a measure of the level of defect or deterioration when compared to their healthy values.

A. Two-port model reconstruction approach

We start by extracting the converter's transient terminal measurements. As explained in the previous section, we consider four pairs of source-load combinations producing distinct transient responses, so the input and output voltages and currents for the k-th measurement set are defined as $v_{in,k}(t)$, $v_{out,k}(t)$, $i_{in,k}(t)$ and $i_{out,k}(t)$ (see Fig. 7). Then, we transform them to the Laplace domain by means of the numerical Laplace transform as follows [17]:

$$[V_{in,k}(s)\ V_{out,k}(s)] = \text{NLT}\{[v_{in,k}(t)\ v_{out,k}(t)]\}, \quad (3)$$

$$[I_{in,k}(s)\ I_{out,k}(s)] = \text{NLT}\{[i_{in,k}(t)\ i_{out,k}(t)]\}, \quad (4)$$

where s is the Laplace variable. More details of the NLT are provided in the Appendix.

For any set of input-output conditions, the following two-port admittance relationship can be defined:

$$\begin{bmatrix} I_{in,k} \\ I_{out,k} \end{bmatrix} = \begin{bmatrix} y_{11}(s) & y_{12}(s) \\ y_{21}(s) & y_{22}(s) \end{bmatrix} \begin{bmatrix} V_{in,k} \\ V_{out,k} \end{bmatrix}, \quad (5)$$

where $y_{11}(s)$, $y_{12}(s)$, $y_{21}(s)$ and $y_{22}(s)$ are the elements of the admittance matrix of the converter. Notice that, conversely to the common definition of an admittance matrix, we consider an asymmetrical matrix for a switching converter model with 4 distinct components, as explained in [16]. To obtain an approximate solution for the 4 admittance elements as a function of the input and output voltages and currents, we define the following overdetermined system consisting of 8 equations with 4 unknowns:

$$\begin{bmatrix} \mathbf{I}_1 \\ \mathbf{I}_2 \\ \mathbf{I}_3 \\ \mathbf{I}_4 \end{bmatrix}_{8\times1} = \begin{bmatrix} \mathbf{V}_1 \\ \mathbf{V}_2 \\ \mathbf{V}_3 \\ \mathbf{V}_4 \end{bmatrix}_{8\times4} [\mathbf{Y}]_{4\times1}, \quad (6)$$

where:

$$\mathbf{I}_k = \begin{bmatrix} I_{in,k} \\ I_{out,k} \end{bmatrix}, \quad (7a) \qquad \mathbf{V}_k = \begin{bmatrix} V_{in,k} & V_{out,k} & 0 & 0 \\ 0 & 0 & V_{in,k} & V_{out,k} \end{bmatrix}, \quad (7b)$$

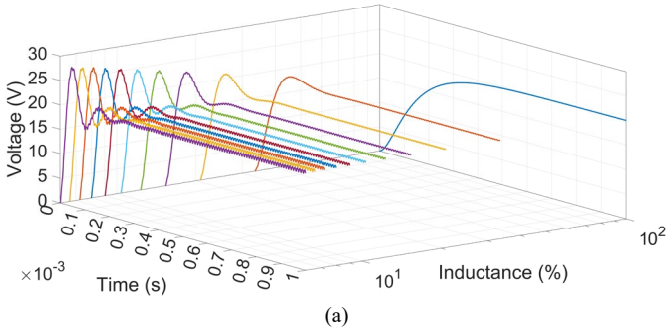

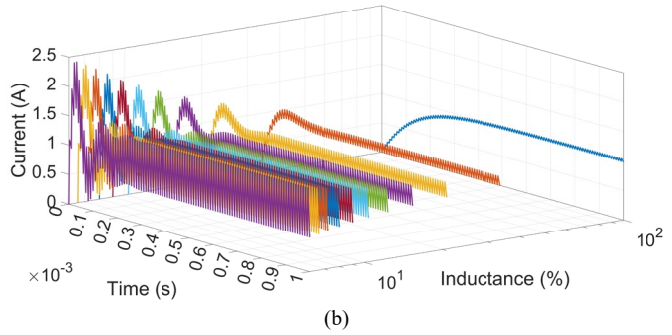

Fig. 5. Transient responses of the DC-DC buck converter for a DC voltage source of 80 V and a load of 20 ohms, considering a decrease of inductance due to widening core fracture: (a) output voltage (b) inductor current.

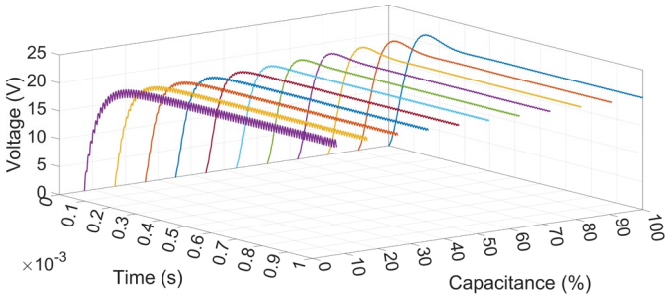

Fig. 6. Output transient voltages of the DC-DC buck converter for a DC voltage source of 80 V and a load of 20 ohms, considering a decrease of capacitance due to premature deterioration, combined with partial inductor core fracture.

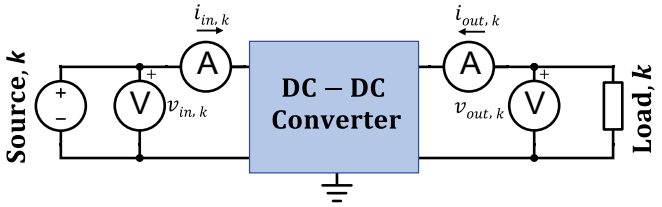

Fig. 7. Measurement arrangement for two-port converter modeling [16]

$$\mathbf{Y} = \begin{bmatrix} y_{11}(s) \\ y_{12}(s) \\ y_{21}(s) \\ y_{22}(s) \end{bmatrix}. \quad (7c)$$

Eq. (6) is solved using the minimum norm least-squares (MNLS) method, which calculates the admittance vector **Y** that minimizes ||**VY**-**I**||. More details and evaluation of this method can be found in [16].

B. Parameter estimation

In order to estimate the inductance and capacitance of the converter, the two-port model in (5) is compared with its analytical approximation in the Laplace domain, as defined in [16], resulting in the following relationships for a buck converter:

$$y_{12,buck} = -d/(sL_{buck}), \tag{8a}$$

$$y_{22,buck} = 1/(sL_{buck}) + sC_{buck}, \tag{8b}$$

and for a boost converter:

$$y_{12,boost} = -(1-d)/(sL_{boost}), \tag{9a}$$

$$y_{22,boost} = (1-d)^2/(sL_{boost}) + sC_{boost}. \tag{9b}$$

Solving for the L-C parameters we obtain the following:

$$L_{buck} = -d/(s\, y_{12,buck}), \tag{10a}$$

$$L_{boost} = -(1-d)/(s\, y_{12,boost}), \tag{10b}$$

$$C_{buck} = y_{22,buck}/s - 1/(s^2 L_{buck}), \tag{10c}$$

$$C_{boost} = y_{22,boost}/\mathrm{s} - (1-d)^2/(s^2 L_{boost}), \tag{10d}$$

where d is the duty cycle of the corresponding converter. This method is applied in the following section to estimate defects in inductors and degradation of capacitors from transient terminal measurements.

VI. Tests Cases

The cases below are intended to evaluate the capability and accuracy of the proposed method in estimating the effects of widening and deepening defects in toroidal inductors, as well as time-based degradation of electrolytic capacitors, for both buck and boost converters.

The parameters of the converter for the test cases are listed in Table I, with initial (healthy) inductor and capacitor values of 3 mH and 1.5 µF for the buck converter, and 1 mH and 40 µF for the boost converter.

For the evaluation of widening and deepening inductor core fractures, as well as capacitor degradation, the parameters and ranges described in Section IV are considered, with 11 values (of L or C) considered for each measurement set.

For the application of the NLT as described in the Appendix, the observation time T is defined as 2.5 ms and the number of samples N is fixed at 40000 for all the cases evaluated in this section.

Fig. 8 shows the results obtained for the buck converter. The parameter estimation for inductance variation as a function of widening and deepening core fractures (Figs. 8(a) and 8(b), respectively) evidences a very accurate reconstruction, with maximum relative deviations below 0.018%. Estimation for the premature capacitance deterioration also shows good agreement with the actual values for the 11 values evaluated, although the largest relative deviation in this case reaches approximately 1.5%.

The results for the boost converter (Fig. 9) closely resemble those from the buck converter. In this case, the max. relative deviation for inductance variation and capacitance deterioration is below 0.04% and 1%, respectively.

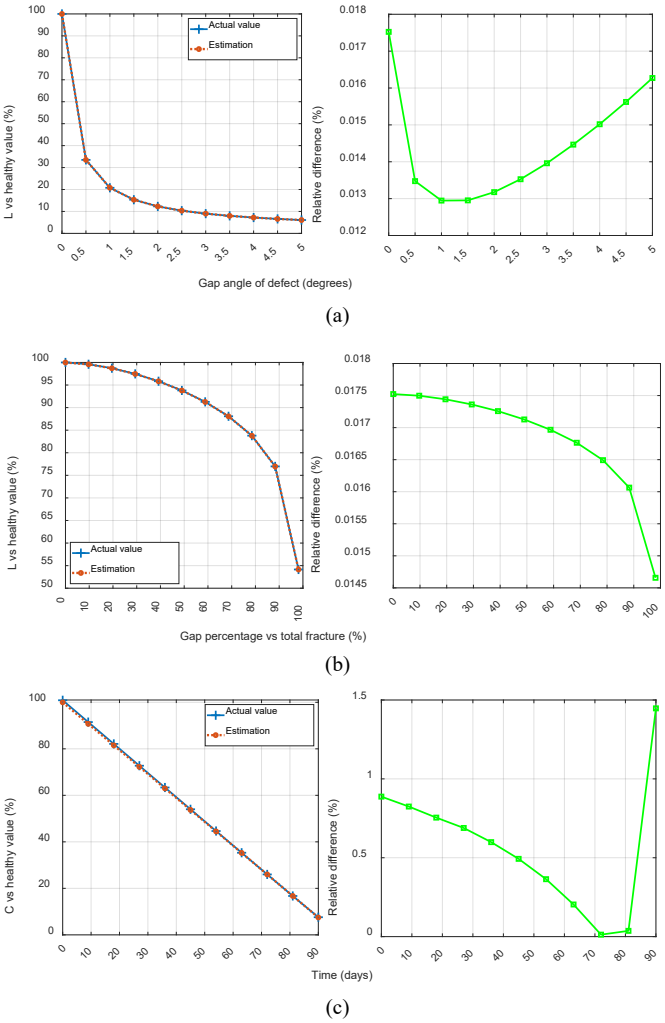

Fig. 8. Results of the proposed parameter estimation method as a function of defect/degradation severity for buck converter: (a) widening core defect in toroidal inductor, (b) deepening core defect of toroidal inductor, (c) premature degradation of electrolytic capacitor.

The reason for larger differences in capacitive parameters when compared to inductive parameters is attributed to the fact that transient terminal responses exhibit more noticeable changes when inductance decreases than when capacitance does, thus allowing a better distinction of the parameter variation responsible for each transient response. Still, the differences presented for the capacitance estimation are considered acceptable for practical purposes.

VII. Conclusions

This paper introduced a novel method to utilize transient terminal responses of DC-DC converters to detect passive parameter variation due to component defect or degradation. This is intended to support the detection of incipient (soft) faults before they become catastrophic to the converter. The proposed method relies on the use of the numerical Laplace transform to obtain frequency domain signals utilized for the reconstruction of a two-port admittance model that, once compared to its analytical version in the Laplace domain, allows the extraction of passive parameters (L and C) for different parameter variation conditions.

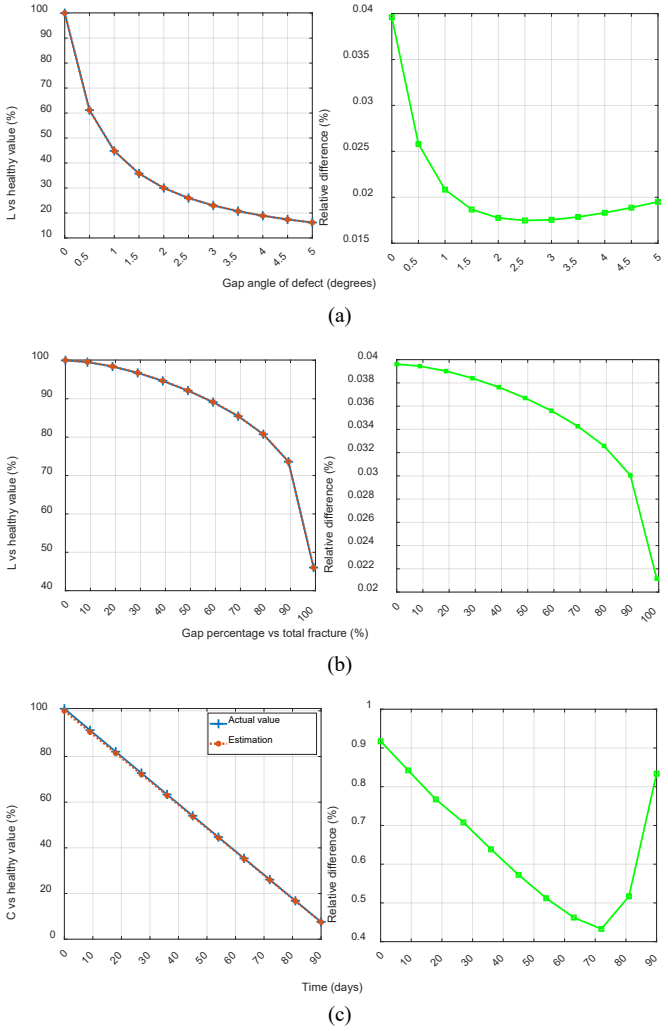

Fig. 9. Results of the proposed parameter estimation method as a function of defect/degradation severity for boost converter: (a) widening core defect in toroidal inductor, (b) deepening core defect of toroidal inductor, (c) premature degradation of electrolytic capacitor.

The results obtained for both buck and boost converter are very satisfactory, showing extremely accurate estimation of inductive parameters exposed to two types of core defects, with relative deviations below 0.05% with respect to the actual values for a series of tests with increasing levels of component defect. For capacitance estimation with respect to time-based component deterioration, the results are also very promising, with maximum relative deviations in the order of 1 to 1.5%.

Future work should include extensive evaluation of this methodology using actual experimental measurements, rather than emulated ones, to get a better understanding of how the proposed method performs with realistic inputs. Additionally, extension to other converters, such as inverters, rectifiers and bidirectional converters, can be explored.

Overall, our proposed method has potential application for different topologies that integrate inductive and capacitive components and can be represented as two-port models in the Laplace domain. For instance, it could be applied to estimate the degradation/damage of filtering stages that include inductive and capacitive components, such as LCL inverter filters used for DER integration.

APPENDIX – NUMERICAL LAPLACE TRANSFORM

This Appendix provides brief definitions of the numerical Laplace transform (NLT), which is applied in this work to convert time domain voltages and currents to the Laplace domain. More details of this technique can be found in [17].

The application of the Laplace transform to a real and causal function $f(t)$ with an observation time T results in its Laplace domain image $F(s)$ as follows:

$$F(s) = \int_0^T [f(t)e^{-ct}]e^{-j\omega t}\, dt, \tag{A.1}$$

where $s = c + j\omega$. The numerical form of (A.1), following an odd sampling of the frequency spectrum, is given by

$$F_m = \sum_{n=0}^{N-1} f_n D_n \exp\left(-\frac{j2\pi mn}{N}\right), \tag{A.2}$$

where

$$m, n = 0, 1, 2 \ldots, N-1, \tag{A.3}$$

$$F_m = F[c + j(2m+1)\Delta\omega], \tag{A.4}$$

$$f_n = f(n\Delta t), \tag{A.5}$$

$$D_n = \Delta t \exp\left(-cn\Delta t - \frac{j\pi n}{N}\right), \tag{A.6}$$

$$\Delta t = \frac{T}{N},\ \Delta\omega = \frac{\pi}{T}, \tag{A.7a,b}$$

$$c = -\ln(10^{-4})/T. \tag{A.8}$$

In (A.3)-(A.8), $\Delta\omega$ is the integration step of the angular frequency ω for odd sampling, Δt is the discrete time step, N is the number of samples, and c is a damping factor included to minimize the aliasing errors produced by the discretization of the frequency spectrum.

VIII. REFERENCES

[1] S. Peyghami, Z. Wang and F. Blaabjerg, "A Guideline for Reliability Prediction in Power Electronic Converters," *IEEE Transactions on Power Electronics*, vol. 35, no. 10, pp. 10958-10968, Oct. 2020.

[2] A. A. Memon, M. Karimi and K. Kauhaniemi, "Evaluation of New Grid Codes for Converter-Based DERs From the Perspective of AC Microgrid Protection," *IEEE Access*, vol. 10, pp. 127005-127030, 2022.

[3] A. Abuelnaga, M. Narimani and A. S. Bahman, "A Review on IGBT Module Failure Modes and Lifetime Testing," *IEEE Access*, vol. 9, pp. 9643-9663, 2021

[4] V. Mariani, et al., "A Survey on Anomalies and Faults That May Impact the Reliability of Renewable-Based Power Systems," *Sustainability*, vol. 16, no. 14, pp. 1-29, 2024

[5] S. Rahimpour, H. Tarzamni, N. V. Kurdkandi, O. Husev, D. Vinnikov and F. Tahami, "An Overview of Lifetime Management of Power Electronic Converters," *IEEE Access*, vol. 10, pp. 109688-109711, 2022

[6] K. Yue, Y. Liu, P. Zhao, B. Wang, M. Fu and H. Wang, "Dynamic State Estimation Enabled Health Indicator for Parametric Fault Detection in Switching Power Converters," *IEEE Access*, vol. 9, pp. 33224-33234, 2021

[7] Z. Gao, C. Cecati and S. X. Ding, "A Survey of Fault Diagnosis and Fault-Tolerant Techniques—Part I: Fault Diagnosis with Model-Based and Signal-Based Approaches," *IEEE Transactions on Industrial Electronics*, vol. 62, no. 6, pp. 3757-3767, June 2015

[8] Z. Gao, C. Cecati and S. X. Ding, "A Survey of Fault Diagnosis and Fault-Tolerant Techniques—Part II: Fault Diagnosis with Knowledge-Based and Hybrid/Active Approaches," *IEEE Transactions on Industrial Electronics*, vol. 62, no. 6, pp. 3768-3774, June 2015

[9] J. Poon, P. Jain, I. C. Konstantakopoulos, C. Spanos, S. K. Panda and S. R. Sanders, "Model-Based Fault Detection and Identification for Switching Power Converters," *IEEE Transactions on Power Electronics*, vol. 32, no. 2, pp. 1419-1430, Feb. 2017

[10] A. Al-Mohamad, G. Hoblos and V. Puig, "A Model-Based Prognostics Approach for RUL Forecasting of a Degraded DC-DC Converter," *2019 4th Conference on Control and Fault Tolerant Systems (SysTol)*, Casablanca, Morocco, 2019, pp. 312-318

[11] F. Bento and A. J. Marques Cardoso, "Fault diagnosis in DC-DC converters using a time-domain analysis of the reference current error," *IECON 2017 - 43rd Annual Conference of the IEEE Industrial Electronics Society*, Beijing, China, 2017, pp. 5060-5065
[12] P. Li, X. Li, and T. Zeng, "A Fast and Simple Fault Diagnosis Method for Interleaved DC-DC Converters Based on Output Voltage Analysis," *Electronics*, vol. 10, pp. 1-14, 2021.
[13] M. Bindi, et al., "Machine Learning-Based Monitoring of DC-DC Converters in Photovoltaic Applications," *Algorithms*, vol. 15, no. 3, pp. 1-18, 2022.
[14] Y. Yu, Y. Jiang, Y. Liu and X. Peng, "Incipient fault diagnosis method for DC–DC converters based on sensitive fault features," *IET Power Electronics*, vol. 13, no. 19, pp. 4646-4658, 2020.
[15] D. R. Espinoza-Trejo, L. M. Castro, E. Bárcenas and J. P. Sánchez, "Data-Driven Switch Fault Diagnosis for DC/DC Boost Converters in Photovoltaic Applications," *IEEE Transactions on Industrial Electronics*, vol. 71, no. 2, pp. 1631-1640, Feb. 2024
[16] H. Alameri, P. Gomez, "Analytical and measurement-based wideband two-port modeling of DC-DC converters for electromagnetic transient studies", *Electric Power Systems Research*, vol. 220, July 2023
[17] P. Gómez, F. A. Uribe, "The numerical Laplace transform: an accurate technique for analyzing electromagnetic transients on power system devices", *Int. Journal of Electrical Power & Energy Systems*, vol. 31, no. 2-3, pp. 116-123, February-March 2009.
[18] B. Hauke, "Basic Calculation of a Buck Converter's Power Stage (rev. B)," Texas Instruments, 2015. [Online]. Available: https://www.ti.com/lit/an/slva477b/slva477b.pdf
[19] B. Hauke, "Basic Calculation of a Boost Converter's Power Stage (rev. D)," Texas Instruments, 2022. [Online]. Available: https://www.ti.com/lit/an/slva372d/slva372d.pdf
[20] Vicor Corporation, "IND TOR 1.03 DIA 2WASSY DWG", 31742 Assembly Drawing Datasheet, 2005. [Online]. Available: https://www.mouser.com/datasheet/2/685/vcrx_s_a0003190862_1-2290903.pdf
[21] ITG Electronics, "PFC212236A Series", PFC212236A-102K Datasheet, 2024. [Online]. Available: https://www.itg-electronics.com/files/0009f7867bd1c27219aabc2585bb9fa8.pdf
[22] COMSOL Multiphysics Version 6.2, COMSOL, Inc., Burlington, MA, USA, 2024.
[23] A. Gupta, O. P. Yadav, D. DeVoto and Jo. Major, "A Review of Degradation Behavior and Modeling of Capacitors," *2018 ASME International Technical Conference and Exhibition on Packaging and Integration of Electronic and Photonic Microsystems (InterPACK 2018)*, San Francisco, California, USA, August 27–30, 2018.
[24] B. Sun, X. Fan, C. Qian and G. Zhang, "PoF-Simulation-Assisted Reliability Prediction for Electrolytic Capacitor in LED Drivers," *IEEE Transactions on Industrial Electronics*, vol. 63, no. 11, pp. 6726-6735, Nov. 2016
[25] B. Sun, X. J. Fan, C. Yuan, C. Qian, and G. Q. Zhang, "A degradation model of aluminum electrolytic capacitors for LED drivers," *16th Int. Conf. Thermal, Mech. Multi-Phys. Simul. Exp. Microelectron. Microsyst. (EuroSimE)*, Apr. 2015, pp. 1–4
[26] MATLAB/Simulink R2023b, The MathWorks, Inc., Novi, MI, USA, 2023.